VORTEX STRUCTURES IN A NON-EQUILIBRIUM GAS

A.I.Osipov, A.V.Uvarov, N.A.Vinnichenko and **N.A.Roschina**

Moscow State University, Physics Faculty, Leninskiye Gory, MSU, Moscow, 119899, Russia

Vortex structures formation and evolution in a non-equilibrium gas is considered on the example of two problems: the convection in the horizontal cylinder and in system of horizontal coaxial cylinders, and also the structure of Karman vortex street. It is shown, that, unlike the linear regime of vortices propagation [1], in a nonlinear case there is an interaction of vortices with non-equilibrium gas, resulting, on the one hand, to redistribution of thermal flows and change of non-equilibrium gas parameters, and on the other hand, to deformation of vortices. These problems, besides theoretical interest, have also the important practical value at designing laser systems and discharge and for the diagnostics.

1. Natural convection in an annulus between coaxial horizontal cylinders with internal heat generation.

The main problem associated with laser and discharge stability is the increase of translation temperature with the power increase. The increase in temperature leads to acceleration of relaxation processes, non-equilibrium decrease, contraction and breakdown of generation. The convective-flow systems are frequently used to achieve a high power output, but they are bulky and difficult in operation. The search of a new scheme of the organization of the discharge is, therefore, constantly under way. In recent years coaxial waveguides have been extensively used [1, 2]. Advantages of such system are obvious. The axis of the cylinder, where the temperature is maximal, can be effectively cooled. Certainly, there are additional problems related to radiation characteristics of such a laser, but these questions will not be considered in the present paper. The primary attention will be focused upon a problem of the heat transfer. In fact, convection in a system of coaxial cylinders at fixed temperatures of cylinders leads to approximately double increase of a flow, compared with the flow determined only by the heat conductivity [3-5].

The purpose of the present work is to investigate a stationary convective flow in the non-equilibrium annulus between two coaxial cylinders. The simplest model of uniform internal heat generation is considered which enables one to simulate the real energy flow. Temperatures of the cylinders are fixed, but can be different and, therefore, in the absence of the energy generation the problem will be reduced to the well known one [3-5].

Convection in systems with heat generation has been studied for a flat layer with uniform source [6] and taking into account energy pumping into vibrational degrees of freedom [7].

Problems associated with the powerful energy generation in nuclear power engineering have been considered as well [8]. However, the problem considered in this paper has features related to the geometry of the system (by contrast to a flat layer, the mode without movement is impossible here) and to capacities (by contrast to a problem of huge capacities of energy generation, in the problem under consideration the temperature mode on the walls can be adjusted as Ra and Ra_T numbers are independent). Moreover, the geometry of coaxial cylinders has some specific features, and the optimization parameter is the temperature field, and not a Nusselt number (its integrated value in the present case is fixed).

Analysis

The configuration to be studied and the coordinate system are shown in Fig. 1. The fluid is contained between two coaxial cylinders of radii R_i and R_o, which are held at temperatures T_o and T_i. The uniform heat generation Q does not depend on coordinates. Density change in the fluid is neglected everywhere except in the buoyancy, and all other physical properties of the fluid are assumed to be constant (Boussinesq approximation).

We consider a two-dimensional problem, and use the cylindrical coordinates (R, θ), where the angular coordinate θ is measured counter-clockwise with respect to the upward vertical axis which contains the center of the cylinders (Fig.1).
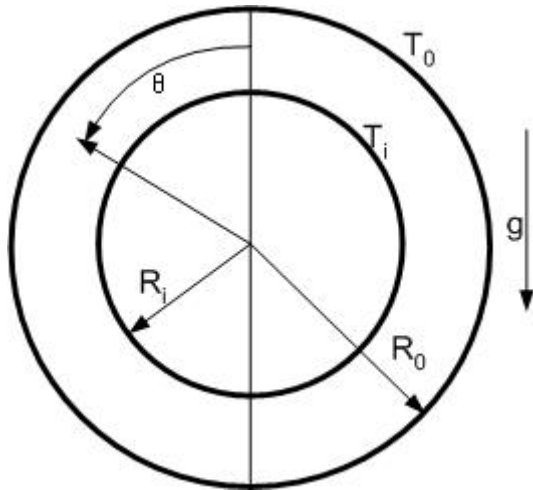

Fig. 1. Geometrical model of the coaxial laser. R_o - radius of the outer cylinder, R_i - radius of the internal cylinder, T_o - temperature on a wall of outer cylinder,
T_i - temperature on a wall of the internal cylinder.

The dimensional governing equations are

$$\frac{\partial U}{\partial R} + \frac{U}{R} + \frac{1}{R}\frac{\partial V}{\partial \theta} = 0, \tag{1.1}$$

$$\rho\left[\frac{\partial U}{\partial t} + U\frac{\partial U}{\partial R} + \frac{V}{R}\frac{\partial U}{\partial \theta} + \frac{V^2}{R}\right] = -\frac{\partial P}{\partial R} + \mu\left[\frac{\partial^2 U}{\partial R^2} + \frac{1}{R}\frac{\partial U}{\partial R} + \frac{1}{R^2}\frac{\partial^2 U}{\partial \theta^2} - \frac{U}{R^2} - \frac{2}{R^2}\frac{\partial V}{\partial \theta}\right] + F_R, \tag{1.2}$$

$$\rho\left[\frac{\partial V}{\partial t}+U\frac{\partial V}{\partial R}+\frac{V}{R}\frac{\partial V}{\partial \theta}+\frac{VU}{R}\right]=-\frac{1}{R}\frac{\partial P}{\partial \theta}+\mu\left[\frac{\partial^2 V}{\partial R^2}+\frac{1}{R}\frac{\partial V}{\partial R}+\frac{1}{R^2}\frac{\partial^2 V}{\partial \theta^2}-\frac{V}{R^2}+\frac{2}{R^2}\frac{\partial U}{\partial \theta}\right]+F_\theta, \quad (1.3)$$

$$\rho c\left[U\frac{\partial T}{\partial R}+\frac{V}{R}\frac{\partial T}{\partial \theta}+\frac{\partial T}{\partial t}\right]+=k\left[\frac{\partial^2 T}{\partial R^2}+\frac{1}{R}\frac{\partial T}{\partial R}+\frac{1}{R^2}\frac{\partial^2 T}{\partial \theta^2}\right]+Q, \quad (1.4)$$

where U and V are the radial and angular velocities, respectively, P is the pressure, T is the temperature, F_R and F_θ are the components of a gravity referred to unit of volume, ρ is a density, μ is the dynamic viscosity, **c** is the thermal capacity referred to a mass unit, **k** is the thermal conductivity.

The temperature constituent of the body-force terms can be written as functions of the temperature difference:

$$F_R = g\rho\beta(T-T_o)\cos\theta \quad (1.5)$$

$$F_\theta = g\rho\beta(T-T_o)\sin\theta, \quad (1.6)$$

where T is the temperature of a fluid in a cavity between cylinders and β is the thermal volume expansion coefficient.

The stream function Ψ can be introduced which satisfies the continuity equation by setting:

$$U = R^{-1}\,\partial\Psi/\partial\theta, \qquad\qquad V = -\partial\Psi/\partial R. \quad (1.7)$$

The dimensionless parameters are

$$\psi = \frac{\Psi}{\alpha}, \qquad r = \frac{R}{L}, \qquad \varphi = \frac{T-T_o}{T_o q}, \qquad u = \frac{UL}{\alpha}, \qquad v = \frac{VL}{\alpha}, \qquad q = \frac{QL^2}{kT_o}, \quad (1.8)$$

where $\alpha = k/\rho c$ is the thermal diffusivity and L=R_o-R_i.

The resulting equations can be simplified by introducing the vorticity ω, defined as:

$$\omega = -\nabla^2\psi, \quad (1.9)$$

where $\nabla^2 = \frac{\partial^2}{\partial r^2}+\frac{1}{r}\frac{\partial}{\partial r}+\frac{1}{r^2}\frac{\partial^2}{\partial \theta^2}$ - laplacian in cylindrical coordinates. $\quad (1.10)$

The initial system (1) - (4) is reduced to dimensionless governing system:

$$\nabla^2\psi = -\omega \quad (1.11)$$

$$\nabla^2 \omega = \frac{1}{Pr}\left[\frac{\partial \omega}{\partial t} + u\frac{\partial \omega}{\partial r} + \frac{v}{r}\frac{\partial \omega}{\partial \theta}\right] + Ra_T\left[\sin\theta\frac{\partial \varphi}{\partial r} + \frac{1}{r}\cos\theta\frac{\partial \varphi}{\partial \theta}\right] \qquad (1.12)$$

$$\nabla^2 \varphi = u\frac{\partial \varphi}{\partial r} + \frac{v}{r}\frac{\partial \varphi}{\partial \theta} - 1 + \frac{\partial \varphi}{\partial t} \qquad (1.13)$$

Where $Pr = \mu c/k$ is the Prandtl number and $Ra_T = \rho g\beta L^3 T_o q/\mu\alpha$ is the modified Rayleigh number.

Temperature and velocity distribution into the annulus between coaxial cylinders are determined by the Prandtl number, Rayleigh number, boundary conditions and geometrical parameters of the system.

In the present problem the boundary conditions correspond to two impermeable isothermal walls of cylinders with constant radii and one vertical symmetry axis at $\theta=0$ and $\theta=180^0$. The stream function is equal to zero on all boundaries along both walls as well as along the symmetry axis as there are no fluxes through the walls and through the plane. The angular derivative temperatures and vorticity on a line of symmetry disappear.

$$\omega = -\partial^2\psi/\partial r^2 \qquad (1.14)$$

The boundary conditions on the symmetry plane become

$$\psi = \omega = \partial\varphi/\partial\theta = 0, \qquad (1.15)$$

While on the inner and outer cylinders they can be written as

$$\psi = u = v = 0 \quad \omega = -\partial^2\psi/\partial r^2 \quad \varphi\big|_{r=ri} = Ra/Ra_T \quad \varphi\big|_{r=ro} = 0. \qquad (1.16)$$

where $Ra = \rho g\beta L^3(T_i - T_o)/\mu\alpha$.

It is possible to use the standard normalization with the parameter $T_i - T_o$ [3-5]. In this case in Eq.(1.12) the parameter Ra_T will be replaced by Ra. In the right hand side of Eq.(13) the unity will be replaced by Ra_T/Ra, and in Eq.(16) for φ one obtains the standard result: $\varphi\big|_{r=ri} = 1 \quad \varphi\big|_{r=ro} = 0$. At both ways of settings results completely coincide. The only exception corresponds to the points where Ra=0 and $Ra_T=0$ because the ratio Ra/Ra_T is not defined and application appropriate of settings is impossible.

At the absence of convection the eq. (13) will be written as:

$$\nabla^2\varphi = -1 \qquad (1.17)$$

with boundary conditions (16). It has the decision:

$$\varphi = -\frac{r^2}{4} + \frac{r_o^2\ln\dfrac{r}{r_i} - r_i^2\ln\dfrac{r}{r_o} - 4\dfrac{Ra}{Ra_T}\ln\dfrac{r}{r_o}}{4\ln r_o/r_i} \qquad (1.18)$$

If to mark $\sigma = \dfrac{2r_i}{r_o - r_i}$ $r_i = \dfrac{\sigma}{2}$; $r_o = 1 + \dfrac{\sigma}{2}$.

The maximum of the temperature will be defined from conditions $\partial\varphi/\partial r = 0$ and corresponded to coordinate $r_{\max}$

$$r_{\max}^2 = \frac{r_o^2 - r_i^2 - 4\dfrac{Ra}{Ra_T}}{2\ln r_o/r_i} = \frac{(1+\sigma) - 4\dfrac{Ra}{Ra_T}}{2\ln\dfrac{2+\sigma}{\sigma}} \tag{1.19}$$

If $r_i < r_{\max} < r_o$, the profile of the temperature is nonmonotonic.

The maximum values appropriate to transition to a monotonous profile, correspond to values $r_{\max} = r_i$ and $r_{\max} = r_o$.

At $r_{\max} = r_i$ from (19) we shall receive

$$\frac{Ra}{Ra_T} = \frac{(1+\sigma) - \dfrac{\sigma^2}{2}\ln\dfrac{2+\sigma}{\sigma^2}}{4} \tag{1.20}$$

At $r_{\max} = r_o$

$$\frac{Ra}{Ra_T} = \frac{(1+\sigma) - 2\left(1+\dfrac{\sigma}{2}\right)^2 \ln\dfrac{2+\sigma}{\sigma^2}}{4} \tag{1.21}$$

The analysis of (1.20) and (1.21) shows, that at the absence of convection the nonmonotonic structure arises only for $\dfrac{Ra}{Ra_T}$ in a range from -0,5 up to 0,5 and faint depends from σ.

Now, setting some initial distributions of temperature and the stream function, using equations (1.11) - (1.13) and boundary conditions (1.15) - (1.16) it is possible to follow the evolution of this initial distribution, and, in particular, to obtain an expression for a limiting stationary mode if it exists. In the numerical solution of our problem we employ the method of final differences. Finite-difference scheme is standard and the Poisson equation (1.11) is solved by the method of variable directions, with the chase method used for every direction.

Results and discussion

The first result is the surface Ra_T (Ra, σ), which separates the region with a two-dimensional convection from the one with the three-dimensional modes. In figure 2 the dependence Ra_T (Ra) for the fixed value $\sigma = 2$ is plotted.
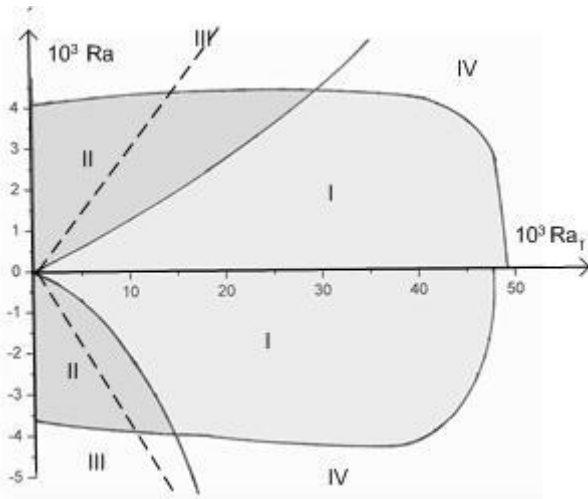
Fig. 2. The dependence Ra (Ra_T) for σ=2.

Four areas have been distinguished. I and II areas correspond to two-dimensional convection, III and IV areas correspond to three-dimensional convection. In the first area (I) convection is accompanied by the formation of two eddies and the temperature gradient varies, however inside each eddy the gradient does not change a mark, while in the second area (II) there is only one eddy and the temperature gradient has one mark.

For comparison the dotted lines separating a range of Ra/Ra_T values from -0,63 to 0,49 are shown in fig.2. In this case in the absence of convection the nonmonotonic temperature profile is observed. These values are calculated under formulas (1.20) and (1.21). As we see the convection reconstructs the temperature structure too much though the existence of a nonmonotonic structure at small values of parameter Ra/Ra_T is kept.

The typical picture of isotherms and streamlines for the first area is represented in fig. 3a, and for the second area is represented in fig. 3b.
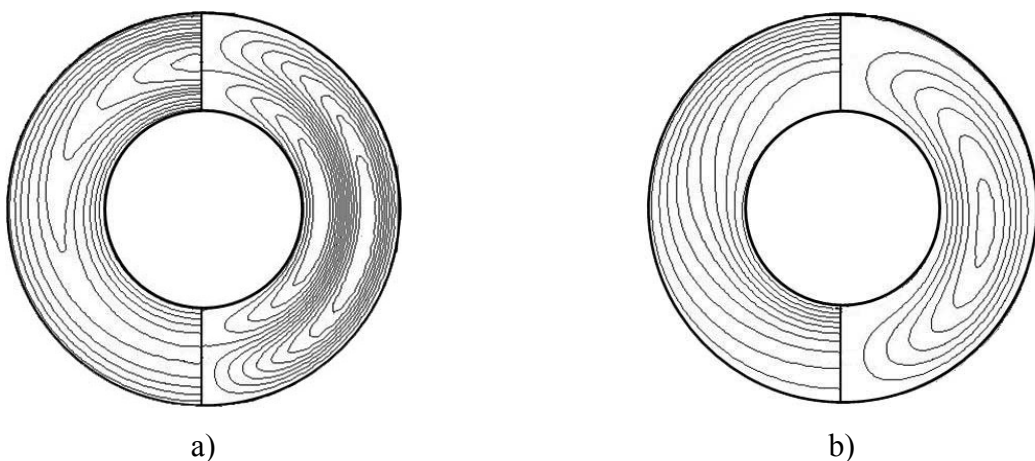

a)   b)

Fig. 3. Isotherms and streamlines for σ =2, a) $Ra = 1 \cdot 10^2$, $Ra_T = 4 \cdot 10^4$ (area I on fig.3). b)

$Ra = 2 \cdot 10^3$, $Ra_T = 5 \cdot 10^3$ (area II on fig.3).

There is only one eddy in the absence of the heat generation in a two-dimensional mode according to a direction of the temperature gradient. The temperature gradient has one mark inside this eddy. The same situation is realized in a problem with the heat generation though the convection changes a range of conditions of the nonmonotonic temperature structure.

There is a disintegration of eddies in the third (III) and the fourth (IV) areas. It corresponds to transition in a new regime, which in the given work was not studied in detail, however well-known for a case of $Ra_T = 0$. There are different two- and three-dimensional structures in this case.

Now let us consider the same system for the prospects of laser construction in the case of equal temperatures on both boundaries (Ra=0).

Now let us compare results without convection. The equation $\nabla^2\varphi = -1$ is readily solved with the boundary conditions $\varphi\big|_{r_i,r_o} = 0$:

$$\varphi = -\frac{r^2}{4} + \frac{r_o^2 \ln{r}/{r_i} - r_i^2 \ln{r}/{r_o}}{4\ln{r_o}/{r_i}} \tag{22}$$

In limit when $\sigma \to 0$ we shall receive the value 0,25 in a maximum which corresponds to a problem with the heat generation for the cylinder when $\varphi = (r_o^2 - r^2)/4$. The coaxial geometry, in comparison with cylindrical, allows to lower twice the maximal temperature in system. The maximal temperature quickly falls down with σ and poorly differs from limiting value 0,125 when $\sigma \geq 1$. We shall consider now a problem with the account of convection.

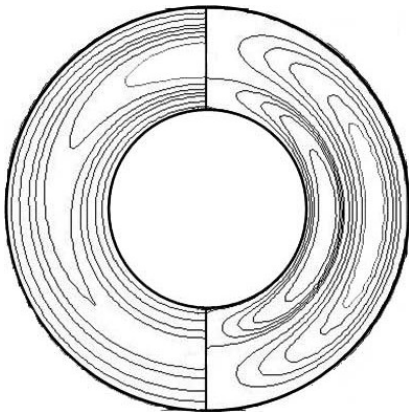Streamlines and isotherms for $\sigma = 2\; r_i = 1\; r_o = 2$, $Ra_T = 3,5\cdot10^4$ are shown in figure 5.

Fig. 5. Isotherms and streamlines when σ=2, Ra$_T$ = 3,5·10^4.

As we can see from the picture, there is a strong heterogeneity of temperature distribution by the angle. The maximal value of temperature exceeds the appropriate maximal temperature value for the no convective case. There are dependences of the maximal temperature achievable

in system from modified Rayleigh number at different values of σ in fig. 6. The maximal temperature value grows with the increasing of Ra_T for the coaxial cylinders system.
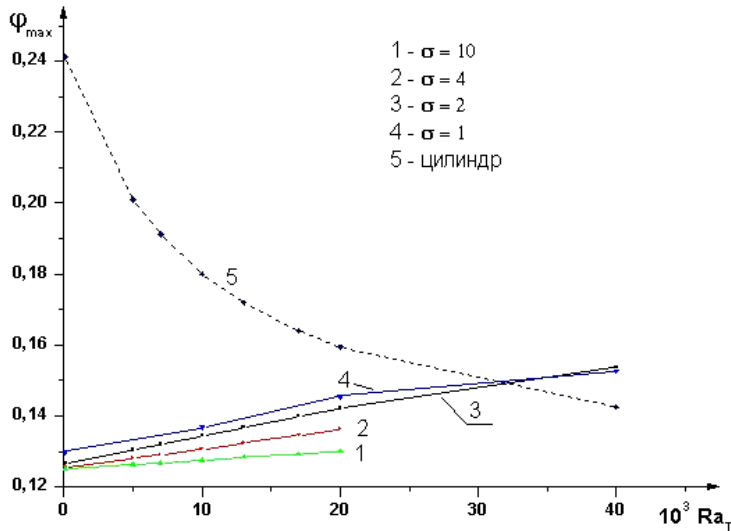

1 - σ = 10
2 - σ = 4
3 - σ = 2
4 - σ = 1
5 - цилиндр

Fig. 6. The maximal temperature from Ra_T at different values of σ.

The heterogeneity of the temperature distribution by the angle can be characterized by the angular heterogeneity of the thermal flows on a wall. If we break the surface on the two half, for the $\sigma = 2$ at $Ra_T = 3,5 \cdot 10^4$, that corresponds to fig. 5, Nusselt numbers are:

$$\int_0^{\pi/2} r \frac{\partial \varphi}{\partial r}\bigg|_{r=ro} = 1,52, \qquad \int_{\pi/2}^{\pi} r \frac{\partial \varphi}{\partial r}\bigg|_{r=ro} = 1,29.$$

$$\int_0^{\pi/2} r \frac{\partial \varphi}{\partial r}\bigg|_{r=ri} = 0,92, \qquad \int_{\pi/2}^{\pi} r \frac{\partial \varphi}{\partial r}\bigg|_{r=ri} = 0,86.$$

Certainly, the total value of the flow thus is kept. It depends only on σ and is equal to $\pi(1 + \sigma)/2$ for the semi-circumference.

The problem with the volumetric heat generation in the cylinder is solved similarly (only in the Cartesian coordinates). There are the typical isotherms and streamlines in the fig.7 and the dependence of the maximal temperature from Ra_T in fig. 6. The temperature falls for the cylinder with increasing of the heat generation and at some value Ra_T it becomes even less, than in a case with coaxial cylinders.

However, it is necessary to recognize, that it is impossible to carry out the direct results comparison, as the Ra_T value is normalized on radius for the cylinder and for coaxial system it is normalized on the wide gap, therefore at the same Ra_T the area of section will be different.

If we consider the same heat generation and area of section the appropriate value of Ra_T for the coaxial cylinder will be much less (namely, in $(1 + \sigma)^{5/2}$ time). However the smaller value of Ra_T means the essential smaller speed of convection (it is necessary to note, as at

identical value of Ra_T the speed of convection is much less in system of coaxial cylinders because of presence of two eddies). Nevertheless, the convection in a two-dimensional case leads in two completely different consequences for the cylinder and the system of coaxial cylinders. In the first case the maximal temperature is strongly reduced while in the second case grows a little. Under the order of size these changes are comparable to a difference of the maximal temperatures at the absence of convection.
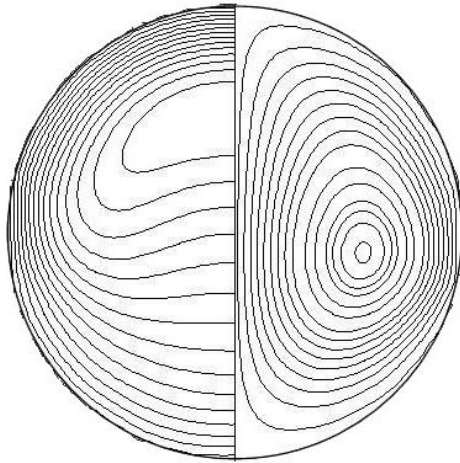

Fig. 7. Isotherms and streamlines for cylinder when Ra$_T$ = 2·10^4.

In the present work we did not consider the limiting transition to the cylinder at the reduction of the radius of the small cylinder. Such geometry is poorly interesting from the practical point of view since it is impossible to provide a constancy of the temperature for the thin cylinder. From the theoretical analysis this transition is not simple because of existence of a return eddy, which covers more area than the internal cylinder area. Even in a case of $\sigma = 0$ the system differs from the cylinder due to existence of the central point with the fixed temperature though the heat flow to the centre in this case aspires to zero.

It is necessary to note, that the calculations given in the present work correspond to a two-dimensional model and to the case of not very high Rayleigh numbers. In addition the model takes into account heat generation in system simply enough. However even this simple model enables one to reveal the basic features of such a system. The structure of the convective currents increase with Ra_T, therefore the analysis of the convective flows plays extremely important role at calculation of geometry of laser system.

The problem of thermal explosion in cylinder can be considered for special form of internal heat generation $Q(T) = Q_0 \exp[b(T - T_0)/T_0]$. The problem for this case of internal heat generation can be solved analytically (Frank-Kamenetskiy (FK) solution without convection). The result of general solution with convection processes is plotted in Fig.8 as the relation of

critical FK parameter with convection to FK parameter without convection. One can see that the intensification of convection processes result in stability of system and the critical parameter increase.
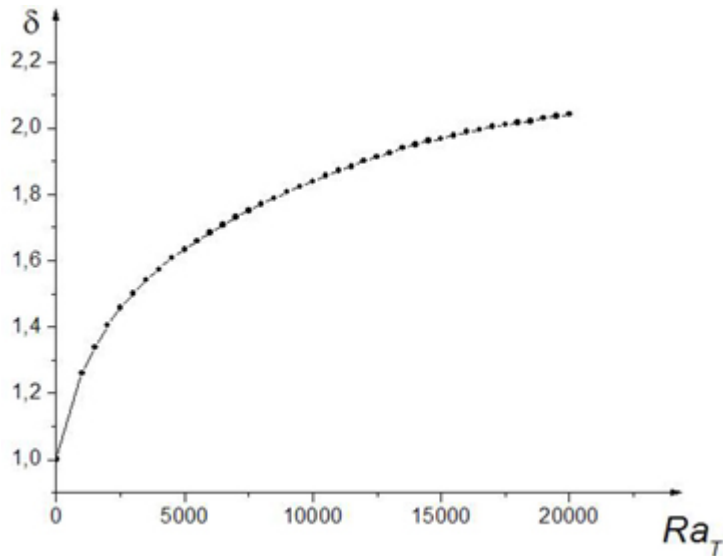

Fig.8. The relation of critical Frank-Kamenetskiy parameter with convection to critical parameter without convection from Ra_T

Conclusions

1. We have considered the problem of convection in a system of two horizontal coaxial cylinders with internal heat generation and different temperatures at the boundaries. The mathematical model which describes the two-dimensional convection has been proposed and the corresponding hydrodynamic parameters have been calculated.

2. The critical surface Ra_T (Ra, σ) which corresponds to a generation of the known results for $Ra_T=0$ has been described.

3. It has been shown that depending on the parameters of a problem there exist two different distributions of two-dimensional currents – with one and two vortices.

4. It has been considered the convection in the horizontal cylinder with a constant heat generation and made comparison of the maximal temperatures at various system geometry. It is shown, that in case of convection in cylinder the maximal temperature reduces with the increasing of heat generation, while in system of coaxial cylinders the maximal temperature increases at not so small radii of the internal cylinder.

2. Influence of non-equilibrium state of medium on the structure of von Karman vortex street.

The problem of non-equilibrium gas flow around a body is quite important for the physics of lasers, astrophysics, and also for solution of the problem of high-speed flight. The

most suitable for the research of vortical flows are the problems, well known in classical hydrodynamics, such as von Karman vortex street, generated by a circular cylinder [9]. The comparison of equilibrium and non-equilibrium gas flows allows to understand the influence of non-equilibrium state and to investigate the essential parameters of the flow. However, the problem of correct choice of model of the medium appears in numerical simulation. More complicated models represent the problem better from physical point of view, but simultaneously the mathematical complexity of simulation is increased. The considered simple problem of the flow around a cylinder allows to evaluate possibility of using simplified models and to understand their boundaries of applicability. Small Mach numbers and moderate (not exceeding 200) Reynolds numbers will be considered.

The existing experimental data [10] use high Reynolds numbers (~ 2000), which are inaccessible for the methods of DNS, used in this paper. Besides, the influence of uncontrolled heat of cylinder surface in experiment is not fully understood, but the comparison with experimental data helps to reveal the fundamental features of relaxation influence on the flow parameters.

Thus, three models of medium will be considered. In the following sections will be described in a parallel way the problem formulation, numerical methods and the results of numerical simulation for three models:

1. The simplest model, taking into account the change in density only in the equation of state but not in the continuity equation. This model is widely used for the analysis of convection (Oberbeck-Boussinesq approximation). The main advantage of this model is that the numerical scheme is stable enough and widely used. The emerging new kinds of scheme allow to improve the accuracy of calculation and the convergence of the method. One of such new varieties of the method will be used in this paper. This model we'll conditionally call «incompressible fluid model».

2. Model, in which an assumption is made that the change in density is generally due to the temperature difference, not the pressure one. This is not typical for the classical hydrodynamics, in which the heat is determined by the square of the velocity, and appears to be small for small Mach numbers. So the compressibility of the medium is taken into account in simplified form. It makes us able to keep the main features of numerical method, used in incompressible fluid model, while increasing the complexity of the algorithm not too much. This model we can call «simplified model of compressible fluid».

3. At last, the complete system of equations for compressible gas with energy release is used. This model can be called «complete model».

1. **Problem formulation.** We consider 2-D flow of viscous vibrationally excited gas around a circular cylinder. For fully compressible fluid the flow is described by the following system of equations, comprising the continuity equation, Navier-Stokes, energy equation, equation of relaxation of non-equilibrium gas and the equation of state.

$$
\begin{cases}
\dfrac{\partial \rho}{\partial t} + div(\rho \cdot \vec{v}) = 0 \\[2mm]
\rho\left(\dfrac{\partial \vec{v}}{\partial t} + (\vec{v}\nabla)\vec{v}\right) = -grad\, p + \eta \Delta \vec{v} + \dfrac{\eta}{3} grad\, div\, \vec{v} \\[2mm]
c_p \rho\left(\dfrac{\partial T}{\partial t} + (\vec{v}\nabla)T\right) = \lambda \Delta T + \dfrac{\eta}{2}\left(\dfrac{\partial v_i}{\partial x_k} + \dfrac{\partial v_k}{\partial x_i} - \dfrac{2}{3}\delta_{ik}\dfrac{\partial v_l}{\partial x_l}\right)^2 + \dfrac{dp}{dt} + \rho\dfrac{\varepsilon - \varepsilon_{eq}(T)}{\tau} \\[2mm]
\rho\left(\dfrac{\partial \varepsilon}{\partial t} + (\vec{v}\nabla)\varepsilon\right) = -\rho\dfrac{\varepsilon - \varepsilon_{eq}(T)}{\tau} + \lambda_v \Delta \varepsilon \\[2mm]
\rho = \dfrac{pm}{kT}
\end{cases}
\quad (2.1)
$$

Here $\mathbf{v}$, ρ, p, T and ε are the velocity, density, pressure, temperature and vibrational energy per unit mass of gas, respectively, η, λ and λ_v are the viscosity, translational and vibrational heat conductivity, c_p is the specific heat at constant pressure, m is the mass of a molecule, k is Boltzmann constant, τ is relaxation time, $\varepsilon_{eq}(T)$ is equilibrium value of vibrational energy, corresponding to temperature T.

As the Mach numbers under consideration are small, the typical relative pressure modification in the flow $\delta p = \rho v^2/(\rho kT/m)$ is small too. Therefore in both the approximate models (the incompressible fluid model and the simplified compressible fluid model) the pressure is supposed constant in the equation of state and energy equation. That is, $\rho \sim 1/T$ and the full derivative of pressure with time is excluded from the energy equation. In the incompressible fluid model density change is also neglected in the continuity equation, which takes the form $div\, \vec{v} = 0$, and the compressible term in energy equation too. In the complete model the entire system of equations is used without any approximations.

In all three models no-slip boundary conditions are used on the cylinder surface, Dirichlet conditions at the inflow boundary, absence of perturbation of the free flow by the cylinder conditions at the lateral boundaries and soft boundary conditions at the outflow boundary. As far as the free stream is relaxational one, the boundary conditions should correspond to the solution of non-equilibrium flow problem in the absence of cylinder. The softness of boundary conditions at the outflow is essential to provide the vortices pass without any reflection. For determination of cylinder temperature the condition of heating up to the temperature of the flow is used, i.e.

$\partial T/\partial n=0$. As far as the conditions of heterogeneous relaxation on the surface of cylinder in the experiment are unknown, two extreme cases of these conditions are considered, that allows to evaluate their influence on the flow parameters. Extreme cases of heterogeneous relaxation correspond to the conditions $\varepsilon=\varepsilon_{eq}(T)$ (infinitely fast heterogeneous relaxation) and $\partial\varepsilon/\partial n=0$ (the absence of heterogeneous relaxation) at the cylinder boundary. In case of complete model, where a boundary condition for the pressure is also needed, a common version is used: $\partial p/\partial n=0$.

     2. Numerical methods. In all of these models an immersed-boundary method was used [11], in order to perform calculation using cartesian grid without complicating the algorithm and simultaneously to satisfy boundary conditions on the cylinder surface by introducing into equations some additional terms, expressing these boundary conditions. We'll demonstrate these terms on the example of incompressible fluid model.

$$
\begin{cases}
div\,\mathbf{v}_1 = q \\[2mm]
\dfrac{\partial \mathbf{v}_1}{\partial t} + (\mathbf{v}_1\nabla)\mathbf{v}_1 = -\dfrac{1}{\rho_1}grad\,p_1 + \dfrac{1}{\text{Re}}\cdot\dfrac{1}{\rho_1}\Delta\mathbf{v}_1 + \mathbf{f} \\[2mm]
\dfrac{\partial T_1}{\partial t} + (\mathbf{v}_1\nabla)T_1 + \dfrac{\varepsilon_0}{c_p\cdot T_0}\dfrac{d\varepsilon_1}{dt} = \dfrac{1}{\text{Pr}\cdot\text{Re}}\cdot\dfrac{1}{\rho_1}\Delta T_1 + g \\[2mm]
\dfrac{d\varepsilon_1}{dt} = -\dfrac{x_0}{V_0}\cdot\dfrac{\varepsilon_1-\varepsilon_{eq}(T_1)}{\tau} + \dfrac{\lambda_v}{x_0 V_0}\cdot\dfrac{1}{\rho_1}\Delta\varepsilon_1 + h \\[2mm]
\rho_1 = \dfrac{p_0 m}{\rho_0 k T_0}\cdot\dfrac{1}{T_1}
\end{cases}
\qquad (2.2)
$$

 (The equations are given in non-dimensional form, with x_0 the diameter of cylinder, V_0, ρ_0, T_0, p_0, ε_0 the velocity, density, temperature, pressure and vibrational energy of unperturbated flow at the inlet, Re и Pr the numbers of Reynolds and Prandtl, respectively). Just like in [11], the term **f** in Navier-Stokes expresses velocity boundary conditions on the cylinder surface, and the term q in continuity equation compensates small nonphysical mass sources, caused by **f**. Unlike [11], the system contains the equations of energy and relaxation, so another additional terms g and h are introduced to provide boundary conditions for temperature and vibrational energy at cylinder boundary. They are introduced analogous to f. All additional terms are applied only in a thin layer near the cylinder boundary.

     To resolve the system of equations (2.2) in approximation of incompressible fluid a Runge-Kutta scheme is used, close to described in [11], with addition of equations of energy and relaxation, and a fractional-step method for the pressure.

In the simplified model of compressible fluid continuity equation contains a term $\partial\rho/\partial t$, therefore the fractional-step method, based on solving the Poisson equation for correction of pressure and velocity field, is inapplicable. Nevertheless, by having neglected in the energy equation the term dp/dt and by using the equation of state in form $\rho\sim1/T$, for each time step after having solved the equation of relaxation we are able to solve the equation of energy for the temperature and to obtain the new value of density. Then this value is used for approximation of the temporal derivative in continuity equation. Therefore, in this case too we are able to obtain the Poisson equation for pressure correction and to keep the main features of numerical method, used in incompressible fluid model.

In the case of complete model the system of equations (2.1) is reduced to conservative form:

$$
\begin{cases}
\dfrac{\partial\rho}{\partial t}+\dfrac{\partial}{\partial x}\left(\rho\,\mathrm{v}_x\right)+\dfrac{\partial}{\partial y}\left(\rho\,\mathrm{v}_y\right)=0 \\[2mm]
\dfrac{\partial(\rho\,\mathrm{v}_x)}{\partial t}+\dfrac{\partial}{\partial x}\left[\rho\,\mathrm{v}_x^2+p+\dfrac{1}{\mathrm{Re}}\left\{\dfrac{2}{3}div\,\vec{\mathrm{v}}-2\dfrac{\partial\mathrm{v}_x}{\partial x}\right\}\right]+\dfrac{\partial}{\partial y}\left[\rho\,\mathrm{v}_x\mathrm{v}_y-\dfrac{1}{\mathrm{Re}}\left\{\dfrac{\partial\mathrm{v}_x}{\partial y}+\dfrac{\partial\mathrm{v}_y}{\partial x}\right\}\right]+f_x=0 \\[2mm]
\dfrac{\partial(\rho\,\mathrm{v}_y)}{\partial t}+\dfrac{\partial}{\partial x}\left[\rho\,\mathrm{v}_x\mathrm{v}_y-\dfrac{1}{\mathrm{Re}}\left\{\dfrac{\partial\mathrm{v}_x}{\partial y}+\dfrac{\partial\mathrm{v}_y}{\partial x}\right\}\right]+\dfrac{\partial}{\partial y}\left[\rho\,\mathrm{v}_y^2+p+\dfrac{1}{\mathrm{Re}}\left\{\dfrac{2}{3}div\,\vec{\mathrm{v}}-2\dfrac{\partial\mathrm{v}_y}{\partial y}\right\}\right]+f_y=0 \\[2mm]
\dfrac{\partial(\rho E)}{\partial t}+\dfrac{\partial}{\partial x}\left[\mathrm{v}_x(\rho E+p)-\dfrac{1}{\mathrm{Re}}\left\{-\mathrm{v}_x\left(\dfrac{2}{3}div\,\vec{\mathrm{v}}-2\dfrac{\partial\mathrm{v}_x}{\partial x}\right)+\mathrm{v}_y\left(\dfrac{\partial\mathrm{v}_x}{\partial y}+\dfrac{\partial\mathrm{v}_y}{\partial x}\right)+\dfrac{\gamma}{\mathrm{Pr}}\dfrac{\partial e}{\partial x}\right\}\right]+ \\[2mm]
+\dfrac{\partial}{\partial y}\left[\mathrm{v}_y(\rho E+p)-\dfrac{1}{\mathrm{Re}}\left\{\mathrm{v}_x\left(\dfrac{\partial\mathrm{v}_x}{\partial y}+\dfrac{\partial\mathrm{v}_y}{\partial x}\right)-\mathrm{v}_y\left(\dfrac{2}{3}div\,\vec{\mathrm{v}}-2\dfrac{\partial\mathrm{v}_y}{\partial y}\right)+\dfrac{\gamma}{\mathrm{Pr}}\dfrac{\partial e}{\partial y}\right\}\right]+g=0 \\[2mm]
\dfrac{\partial(\rho\varepsilon)}{\partial t}+\dfrac{\partial}{\partial x}\left[\rho\varepsilon\,\mathrm{v}_x-\dfrac{\lambda_\mathrm{v}}{\rho_0\mathrm{V}_0x_0}\dfrac{\partial\varepsilon}{\partial x}\right]+\dfrac{\partial}{\partial y}\left[\rho\varepsilon\,\mathrm{v}_y-\dfrac{\lambda_\mathrm{v}}{\rho_0\mathrm{V}_0x_0}\dfrac{\partial\varepsilon}{\partial y}\right]+h=-\dfrac{x_0}{\mathrm{V}_0\tau}\rho\left(\varepsilon-\varepsilon_{eq}(T)\right) \\[2mm]
p=\dfrac{kT_0}{m\mathrm{V}_0^2}\rho T
\end{cases}
\qquad (2.3)
$$

where

$$E=\frac{c_\mathrm{v}T_0}{\mathrm{V}_0^2}T+\frac{1}{2}\mathrm{v}^2+\frac{\varepsilon_0}{\mathrm{V}_0^2}\varepsilon,\quad e=\frac{c_\mathrm{v}T_0}{\mathrm{V}_0^2}T+\frac{\lambda_\mathrm{v}\varepsilon_0c_\mathrm{v}}{\lambda\mathrm{V}_0^2}\varepsilon,\ \gamma$$ is the specific-heat ratio. To solve the obtained system two-step Lax-Wendroff scheme [12] was used, slightly modified because of the presence of a source term in the right side of equation of relaxation: it is taken into account only on corrector step.

Calculations were carried out using staggered grids 240x170 points, thickening in both directions with approaching to cylinder.

3. Results of numerical simulation. Computations were performed at Re=75, Pr=0.7, T_0=500 K, vibrational temperature of non-equilibrium gas at the inlet 3000 K, relaxation time is

15 times more than the vortex street period, Mach number is about 1/8. This corresponds relaxation only slightly perturbating the basic flow — classical von Karman vortex street — but being large enough in comparison with the effects of compressibility.

Even incompressible fluid model demonstrates the main effects of relaxation influence upon the flow.
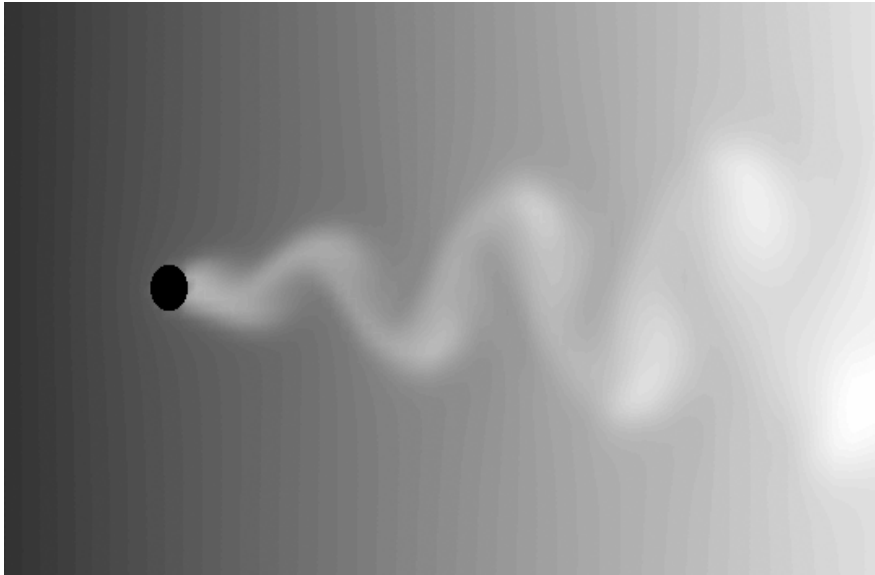

Fig. 9. Temperature distribution. Lighter regions correspond to higher temperatures

As one can see from the Fig.9, Karman street vortices, the gas in which moves longer than the gas in the remaining part of the flow, have time to receive more energy from the vibrational degrees of freedom and, therefore, are heated more than the surrounding flow. Accordingly, density of gas in vortices is diminished, which result in compression of vortex region by the colder and denser surrounding gas. In the experiment [10] the transverse projection of velocity V_y fluctuation spectrum was measured. The compression of vortices causes these fluctuations to damp. But besides the transverse gradient of temperature, there is a longitudinal one: the gas is gradually heated, which lead to decrease of density and Reynolds number, and deformation of the vortices. The vortices become less violent at the centre but more violent on the edges (Fig.10).
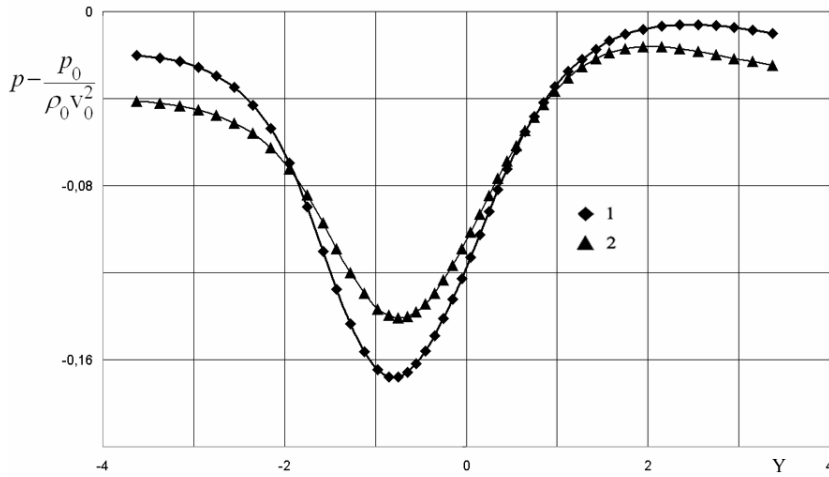
Fig. 10. Modification of pressure distribution along Y-axis due to vortex deformation because of the decrease in Re: 1 — equilibrium gas, 2 — vibrationally excited gas

Influence of this effect on velocity fluctuations depends on the measurement point of these fluctuations, depending on, whether a center of a vortex passes through this point or a vortex edge, the amplitude of the pulsations may both decrease and increase. The total change in velocity pulsations amplitude depends on the ratio of damping and deformation of the vortices in a concrete measurement point and may be of both signs, as it follows from the experiment [10] (Fig.11 a, b).
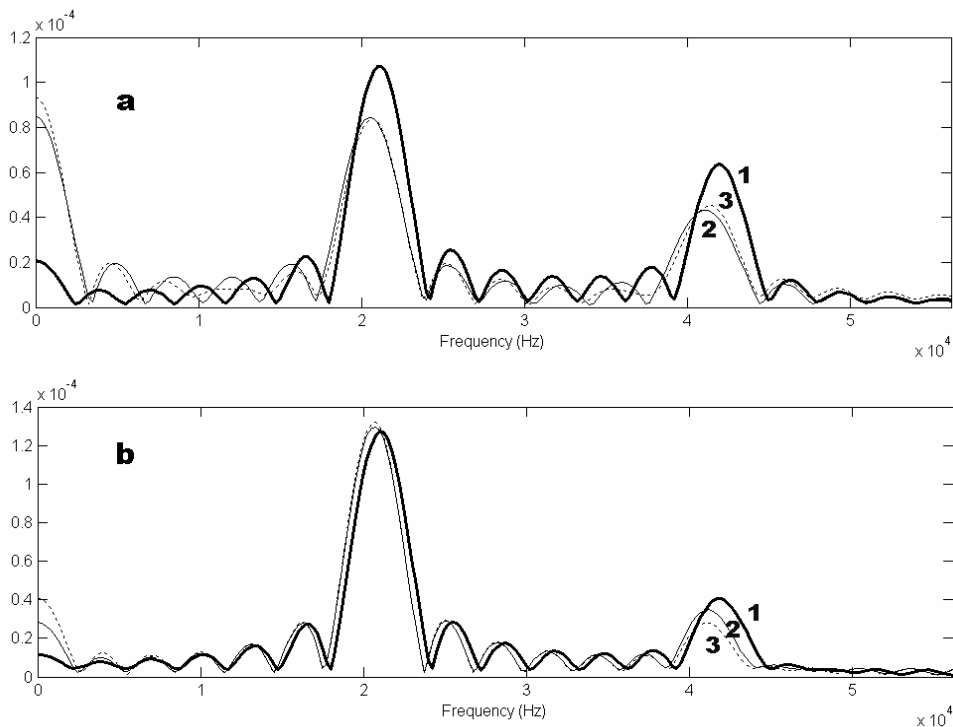

Fig. 11. Modification of velocity fluctuation spectrum: 1 — equilibrium gas, 2 и 3 — non-equilibrium gas with different conditions of heterogeneous relaxation on the cylinder surface

16

As one can see from the spectra, the choice of a condition of heterogeneous relaxation hardly affects the result: the curves 2 and 3 are much closer to each other than to the curve 1, corresponding to equilibrium case. Taking into account the dependence of relaxation time from temperature according to Landau-Teller formula $\tau=A\cdot exp(B/T^{1/3})$ has little influence too. This dependence only increases the temperature contrast between the vortices and the surrounding gas, slightly changing the ratio between two present effects. Another way to introduce non-equilibrium state — constant energy pumping into vibrational degrees of freedom all over the computational domain instead of non-equilibrium state of gas at the inflow — changes the observed phenomena little. With such formulation of the problem at first the gas relaxates little (because it is close to equilibrium), but then, having saved up some vibrational energy, it begins to transfer the energy into translational degrees of freedom as in the case of non-equilibrium gas at the inflow. The influence of energy pumping is not very essential. This pumping only creates the non-equilibrium gas flow not at the inflow border, but more near the cylinder surface. Therefore, though the vibration energy distribution will be changed, the temperature distribution will be the same and the effects of damping and deformation of vortexes will be observed.

In the cases of simplified and complete models of compressible fluid the obtained

distributions do not vary essentially, but the velocity fluctuation spectrum exhibits a shift

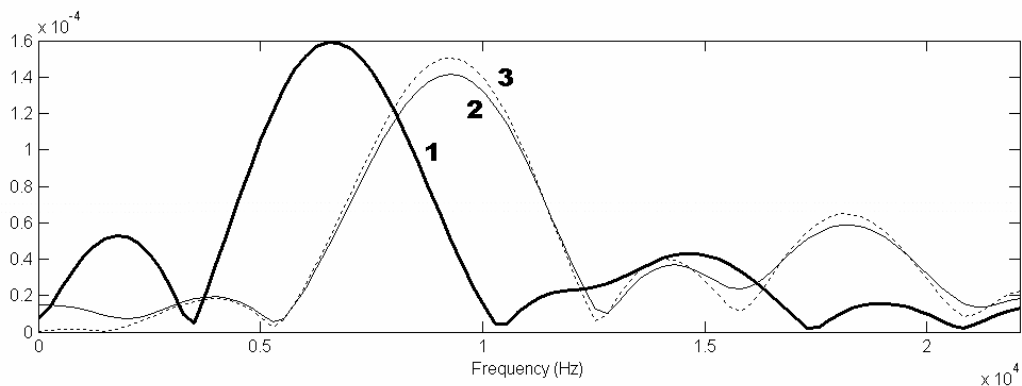towards higher frequencies (Fig. 12).

Fig 12. Velocity fluctuation spectrum for three different models: 1 —

incompressible fluid model, 2 — simplified model of compressible fluid,

3 — complete model   ven at small

Much numbers (1/8). We shall notice, that the shift value, and the entire spectrum are very

similar for these two models in spite of the fact that calculation using the simplified model is

much easier. The frequency shift is present only in case of non-equilibrium compressible gas, in

which the relaxation creates a non-uniform field of density, in which compressibility of gas

results in reduction of distance between vortexes and frequency increase in a spectrum. This fact

corresponds to experiment [10], where frequency shift in non-equilibrium gas was observed in

comparison with the equilibrium case.

Let's emphasize, that in the case of strongly non-equilibrium gas the simplified model yields the results very close to the complete model, but in the case of near-equilibrium gas the discrepancy between two models increases (Figs. 13 a, b).

This result is easy to understand physically. The effects of compressibility and heating due to change of kinetic energy of the flow become of the same order as the relaxation effects. The simplified model describes well the gas heating behind the cylinder, but it is unable to take into account the heating of gas ahead of the cylinder and cooling in zones of expansion at the sides. For strongly non-equilibrium case these effects are small in comparison with relaxation heating, and the simplified model results in correct description, but in case of the gas near equilibrium, the simplified model is inapplicable.
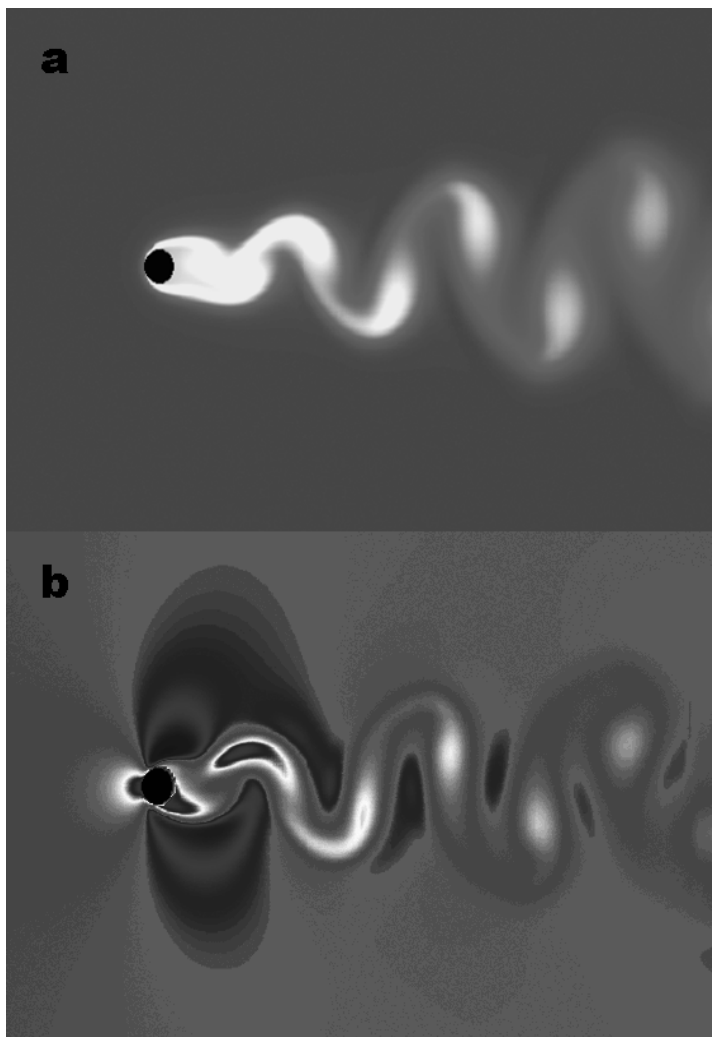

Fig. 13. Temperature field. Near-equilibrium gas: a — simplified model, b — complete model

Conclusions. Numerical simulation of the flow of non-equilibrium gas around a circular cylinder is carried out within the framework of three gas-dynamic models. Distributions of

velocity, temperatures and pressure are obtained, and also the spectrum of pulsations of velocity is calculated.

It is shown, that for strongly non-equilibrium state (the dominance of relaxation effects over those of compressibility) the basic result of influence of non-equilibrium state on the flow in all three models will be damping and deformation of vortexes. The damping of vortexes is the result of relaxation heating of vortexes in comparison with surrounding gas and the corresponding reduction of density in vortexes (the transverse gradient of temperature and density). Deformation (weakening at the center and amplification on edges) is caused by gradual heating of relaxating gas and reduction of density (the longitudinal gradient of temperature and density). The influence of non-equilibrium state on spectrum of velocity pulsations is determined by a ratio of these two factors in a concrete point of observation and it can result in both amplification and damping of the basic frequency that corresponds to experimental data. In comparison with the model of incompressible fluid, the simplified model of compressed fluid and complete model yield a shift in the spectrum towards higher frequencies, caused by influence of effects of compressibility on the non-uniform distribution of density arising as a result of relaxation. It is revealed, that the simplified model demanding considerably smaller calculations, in case of strongly non-equilibrium gas yields the results similar to complete model. However, in the case of a gas near the equilibrium state, the role of compressibility increases, and the simplified model describes the flow insufficiently well. Also it is shown, that the different conditions of heterogeneous relaxation on the cylinder surface and non-equilibrium creation methods poorly influence on the flow.

References

1. Habich U., Plum H-D. Diffusion-cooled CO2 laser with coaxial high frequency excitation and internal axicon. J. Phys. D: Appl. Phys., 1993, **26**, p 183-191.

2. Wang Y., Huang X., Chen Q., Li Z. Coupling efficiencies and mode discrimination in coaxial waveguide laser resonators. J. Phys. D: Appl. Phys., 1999, **32**, p 2613-2619.

3. Kuehn, T.H. and Goldstein, R. J. An experimental and theoretical study of natural convection in the annulus between horizontal concentric cylinders. Journal of fluid Mechanics, 1976, **74**, p 695-719

4. Kumar R. Study of natural convection in horizontal annuli. Int. J. Heat Mass Transfer, 1988, **31**, p 1137-1148

5. Yoo J.-S. Prandtl number effect on bifurcation and dual solutions in natural convection in a horizontal annulus. Int. J. Heat Mass Transfer, 1999, **42**, p 3279-3290

6. Sparrow E.M., Goldstein K.J., Jonsson V.K. Thermal instability in a horizontal fluid layer effect of boundary condition and non-linear temperature profile. J. Fluid Mech., 1964, **18,** № 4, p 513

7. Osipov A.I., Uvarov A.V. Stability problems in a nonequilibrium gas. Physics-Uspekhi, 1996, **39**, № 6, p 597-608

8. Bolshov L.A., Kondratenko P.S., Strizhov V.F. Natural convection in a heat-generating fluid, Physics-Uspekhi, 2001, **44**, №10, p 999-1016

9. Williamson C.H.K. Vortex dynamics in the cylinder wake // Annu. Rev. Fluid Mech. 1996. V. 28. P. 477-539.

10. Gembarzhevskii G.V., Generalov N.A., Solov'ev N.G. Investigation of the velocity fluctuation spectrum of a vortex flow of vibrationally excited molecular gas in a glow discharge // Fluid Dynamics. 2000. V. 35. № 2. P. 222-231.

11. Kim J., Kim D., Choi H. An immersed-boundary finite-volume method for simulations of flow in complex geometries // J. Comput. Phys. 2001. V. 171. № 1. P. 132-150.

12. Richtmyer R.D., Morton K.W. Difference methods for initial-value problems. Interscience Publishers. New York. 1967.